

# SHOT PEENING OF NON-FERROUS ALLOYS TO ENHANCE FATIGUE PERFORMANCE

L. Wagner, M. Wollmann

Institute of Materials Science and Engineering  
Clausthal University of Technology  
Agricolastraße 6, D-38678 Clausthal, Germany

## ABSTRACT

The HCF response to shot peening of the non-ferrous alloys based on magnesium, aluminum and titanium is compared and contrasted. It is shown that magnesium alloys respond quite critically to a variation in Almen intensity. Marked enhancements in fatigue strength were observed after peening only at very low intensities. Aluminum alloys are much more tolerable with regard to Almen intensity since no overpeening effect was observed. Generally, naturally aged conditions (T4) respond to shot peening more beneficially than artificially aged conditions (T6). The response of titanium alloys to shot peening is highly dependent on the alloy class. The  $\alpha$  titanium alloys often respond quite beneficially. In contrast, ( $\alpha+\beta$ ) and in particular, metastable  $\beta$  titanium alloys can exhibit even a loss in fatigue strength after shot peening. Possible explanations for such behavior are outlined in terms of work-hardening capabilities, mean stress and environmental sensitivities of the various materials and microstructural conditions.

## KEY WORDS

Shot peening, light alloys, work-hardening, residual stresses, HCF performance

## INTRODUCTION

Mechanical surface treatments such as shot peening and ball-burnishing are often applied to light alloys based on aluminum and titanium mostly to improve their HCF strengths in aircraft applications. As opposed to these alloys, much less is known regarding the effects of mechanical surface treatments on magnesium based alloys although this lowest weight alloy class is expected to gain much more interest in the future because of increasing concerns regarding fuel consumption in transportation.

In general, the improvement of the fatigue performance of metallic materials can be derived from two contributing factors, namely surface strengthening by the induced high dislocation densities and residual compressive stresses [G. R. Leverant et al. 1979, L. Wagner and G. Lütjering 1982]. While surface strengthening is able to enhance the resistance to fatigue crack nucleation, micro-crack propagation resistances are detrimentally affected owing to low residual ductility in the cold worked and strengthened surface layer. On the other hand, there is experimental evidence that residual compressive stresses can drastically reduce the growth rate of tiny surface cracks in titanium and aluminum alloys [L. Wagner 1989, L. Wagner and C. Müller 1992] while crack nucleation resistances are less affected.

The present investigation is intended to highlight differences in the fatigue response to mechanical surface treatments of the various non-ferrous alloys.

## EXPERIMENTAL

The investigation was performed on the wrought magnesium alloys AZ31 and AZ80, the age-hardenable aluminum alloys Al 6082 and Al 2024, the  $\alpha$ -titanium alloy Ti-2.5Cu, the ( $\alpha+\beta$ ) titanium alloy Ti-6Al-4V and the metastable  $\beta$ -titanium alloy TIMETAL LCB.

Both magnesium alloys were received as extrusions and were tested without further heat treatments. The aluminum alloys were also received as extrusions but were given either natural (T4) or artificial (T6) tempers. The titanium alloy Ti-2.5Cu was received as hot rolled plate and was tested in a fully aged condition. The ( $\alpha+\beta$ ) titanium alloy Ti-6Al-4V was thermomechanically processed to obtain duplex microstructures. The cooling rate from the duplex anneal was varied between water quenching (D/WQ) and air-cooling (D/AC). Material was subsequently aged at 500°C for 24 hours. The metastable  $\beta$  titanium alloy TIMETAL LCB was received as  $\varnothing$  14.3 mm that had been solution heat treated. Various aging treatments were applied with and without a 10% prior pre-strain in tension (PS) which resulted in a wide variation of strength levels [M. Kocan et al. 2005].

Tensile tests were performed on threaded cylindrical specimens having gage lengths and gage diameters of 20 and 4 mm, respectively. The initial strain rate was  $10^{-3}$  s $^{-1}$ . The tensile properties of the various alloys and microstructures are listed in Table 1.

Table 1: Tensile properties of the various light alloys

	$\sigma_{0.2}$ (MPa)	UTS (MPa)	EL (%)
AZ31	210	280	15
AZ80	235	340	12
Al 6082-T4	220	350	21
Al 6082-T6	340	365	12
Al 2024-T4	420	590	16
Al 2024-T6	370	460	11
Ti-2.5Cu	685	770	16
Ti-6Al-4V, D/AC	985	1045	13
Ti-6Al-4V, D/WQ	1060	1110	13
LCB, 0.5h 500°C	1475	1565	8
LCB, 8h 540°C	1180	1210	13
LCB, PS + 0.5h 500°C	1665	1730	3.3

Shot peening was performed using spherically conditioned cut wire having an average shot size of 0.36 mm (SCCW14). In addition, a very hard shot (800 HV0.1) with an average size of 0.6 mm was used. All peening was done to full coverage at various Almen intensities. For comparison, a few specimens were ball-burnished using a hydrostatic tool by which a hardmetal ball ( $\varnothing$ 3 mm) is pressed onto the surface. Microhardness-depth profiles and residual stress-depth profiles as determined by either X-ray diffraction or the incremental hole drilling method were measured to characterize the process-induced changes in surface layer properties.

Fatigue tests in rotating beam loading were performed on hour-glass shaped specimens having a minimum gage diameter of 4 mm. In addition to shot peened and ball-burnished conditions, electrolytically polished specimens were prepared to serve as reference.

## RESULTS AND DISCUSSION

### Magnesium alloys

The microhardness-depth profiles of AZ31 and AZ80 after shot peening with SCCW 14 using an Almen intensity of 0.48 mmN are illustrated in Figure 1 indicating pronounced work-hardening in the near-surface layers. The corresponding residual stress-depth profiles are shown in Figure 2. As expected, the residual compressive stresses in AZ80 are somewhat higher than in AZ31. The penetration depths in AZ80 and the depths where maximum compressive stresses prevail are lower than in AZ31. These results can be explained by the more marked work-hardening and higher strength in AZ80 compared to AZ31 (Table 1).

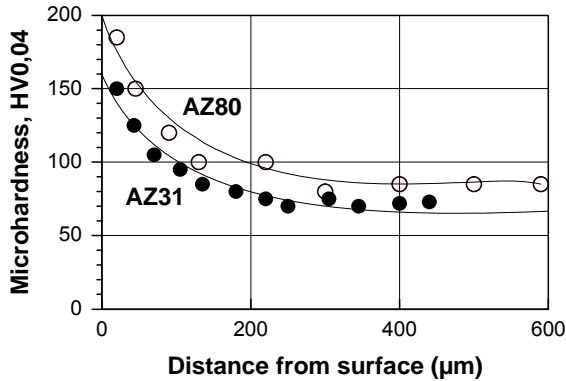


Fig. 1: Microhardness-depth profiles

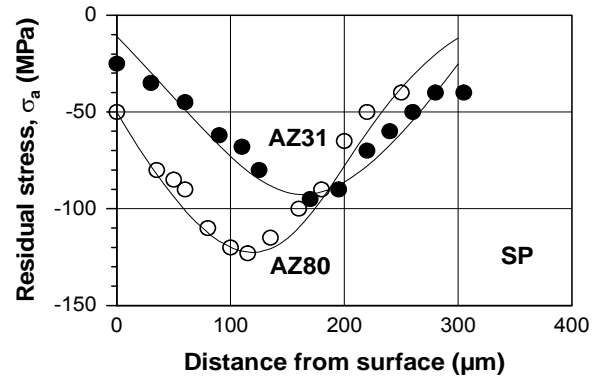
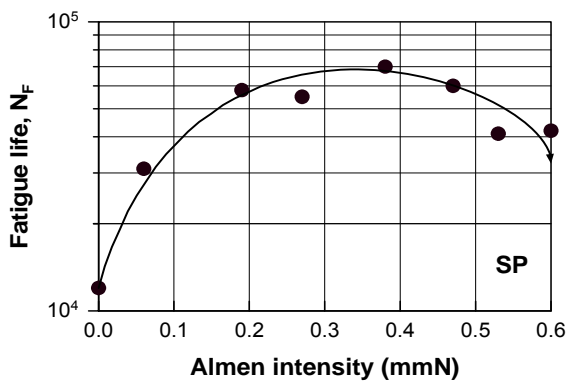
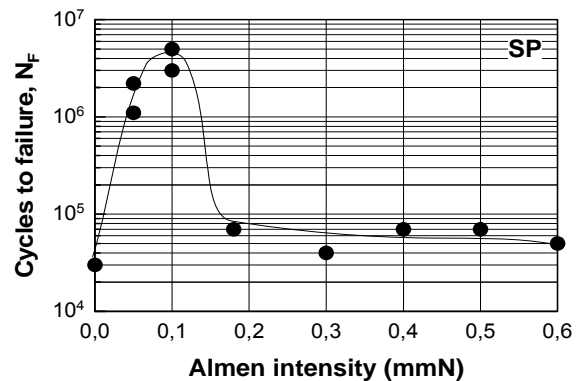


Fig. 2: Residual-stress depth-profiles

With regard to fatigue performance (Fig. 3), both alloys respond quite critically to a variation in Almen intensity, particularly AZ80 (compare Fig. 3b with Fig. 3a).



a) AZ31,  $\sigma_a = 125$  MPa

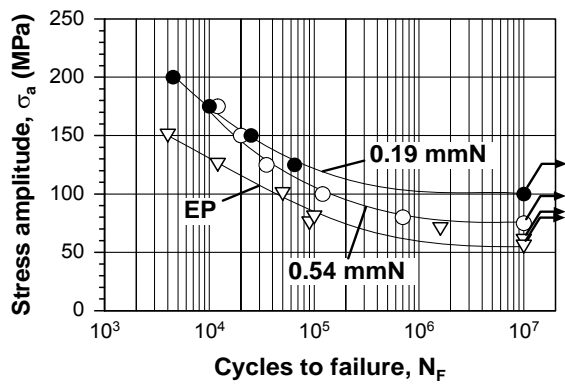


b) AZ80,  $\sigma_a = 175$  MPa

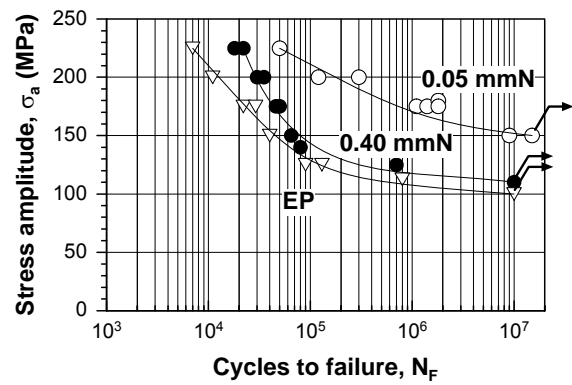
Fig. 3: Fatigue life vs. Almen intensity, rotating beam loading ( $R = -1$ )

Obviously, optimum Almen intensities in the higher strength alloy AZ80 (Fig. 3b) are even lower than those observed in AZ31 (Fig. 3a). However, optimum Almen intensities lead to fatigue life enhancements in AZ80 (Fig. 3b) much more pronounced than in AZ31 (Fig. 3a). By using various shot media (steel shot, ceramic balls, glass beads) and various shot sizes, it was shown (M. Hilpert et al. 1999) that the fatigue life of shot peened AZ80 followed the trend in Fig. 3b, i.e., the fatigue performance was only dependent on Almen intensity.

S-N curves are illustrated in Fig. 4 indicating that on both AZ31 (Fig. 4a) and AZ80 (Fig. 4b) low intensity shot peening leads to fatigue performances markedly superior to high intensity peening.



a) AZ31



b) AZ80

Fig. 4: S-N curves in rotating beam loading ( $R = -1$ )

Presumably, the poor performance of the magnesium alloys after shot peening with high intensities is related to process-induced microcracks. Removing these microcracks by polishing away  $120\ \mu\text{m}$  from the as-peened surface results in a highly improved HCF strength as demonstrated on AZ80 in Figure 5.

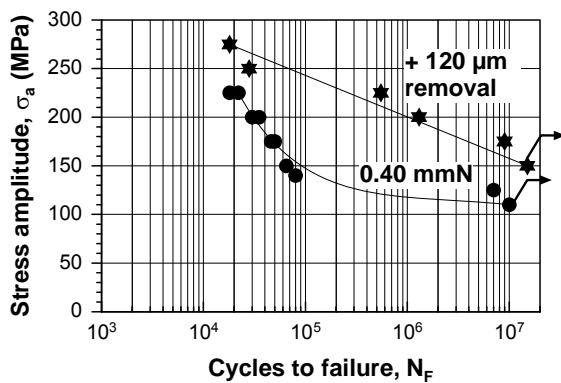


Fig. 5: S-N curves in rotating beam loading ( $R = -1$ )

### Aluminum Alloys

The microhardness-depth profiles after shot peening the aluminum alloys with SCCW14 ( $0.20\ \text{mmA}$ ) are shown in Fig. 6.

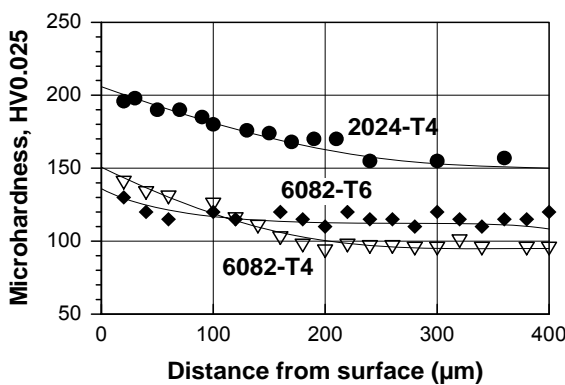


Fig. 6: Microhardness-depth profiles

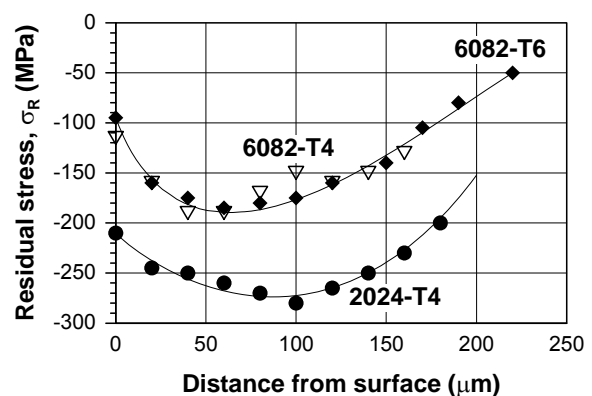


Fig. 7: Residual stress-depth profiles

Both Al 6082-T4 and Al 2024-T4 respond with a marked increase in near-surface hardness while very limited hardness increase was observed on Al 6082-T6. These

results can be explained by the work-hardening capabilities being quite different among the various alloys and conditions (Tab. 1).

Shot peening-induced residual stress depth-profiles are illustrated in Fig. 7. For both Al 6082 and Al 2024-T4, pronounced residual compressive stresses were determined with maximum values in Al 2024-T4 being higher than in the lower strength alloy Al 6082-T4 and 6082-6.

In contrast to the magnesium alloys, no overpeening effect was observed on the aluminum alloys. An example is shown for Al 6082-T6 in Figure 8. The absence of an overpeening effect can be explained by the fcc crystal structure which allows high deformation degrees in the surface layer without inducing microcracks.

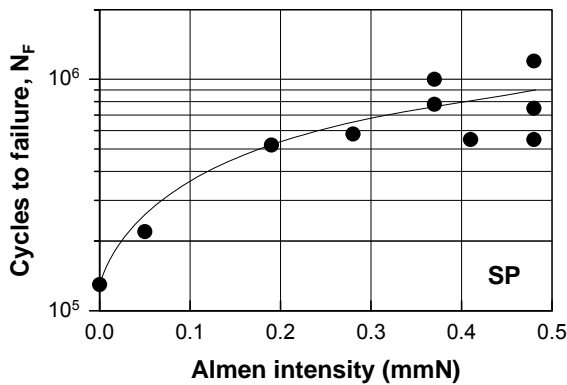


Fig. 8:  $N_F$  vs. Almen intensity

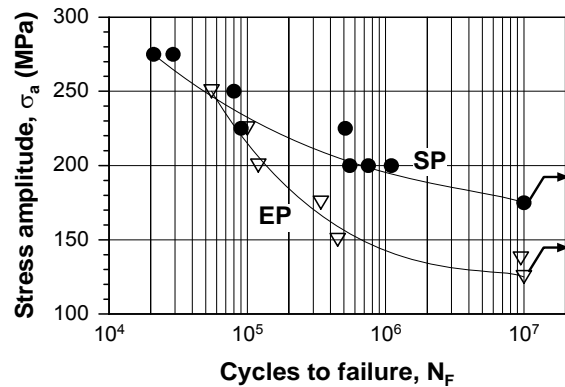
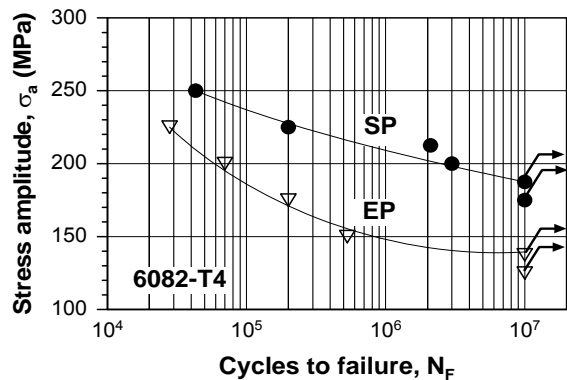
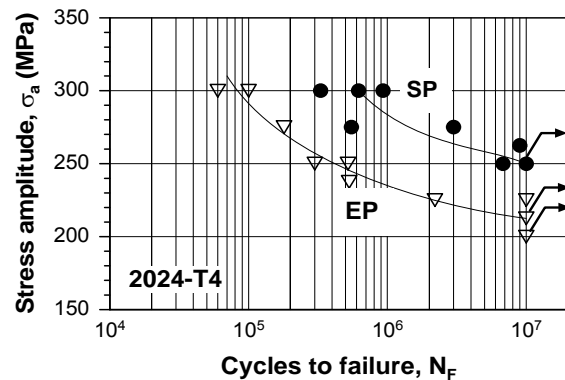


Fig. 9: S-N curves in Al 6082-T6

S-N curves of the shot peened aluminum alloys (0.20 mmA) are illustrated in Figs. 9 and 10 comparing results with electropolished references on Al 6082-T6 (Fig. 9) and Al 6082-T4 (Fig. 10a) and Al 2024-T4 (Fig. 10b).



a) Al 6082-T4



b) Al 2024-T4

Fig. 10: S-N curves in naturally aged aluminium alloys, rotating beam loading ( $R = -1$ )

While there is a significant improvement in HCF performance of the tested alloys and aging conditions by shot peening, there is almost no fatigue life enhancement at high stress amplitudes in Al6082-T6 (Fig. 9). This result may be caused by early residual stress decay in the naturally aged temper.

### Titanium alloys

The microhardness-depth profile on the shot peened (0.20 mmA)  $\alpha$ -titanium alloy Ti-2.5Cu is shown in Fig. 11 illustrating marked work-hardening as also seen in Table 1. The corresponding residual stress-depth profile is plotted in Fig. 12 indicating

pronounced compressive stresses with maximum values below the shot peened surface.

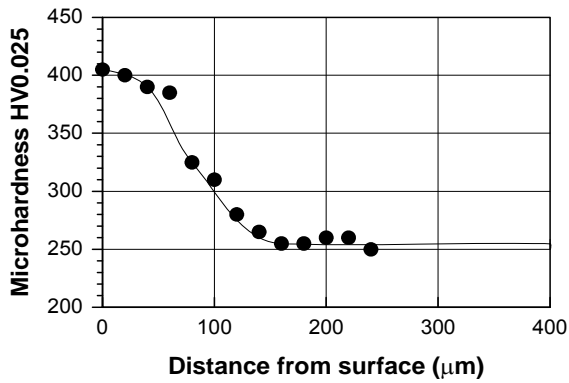


Fig. 11: Microhardness-depth profile

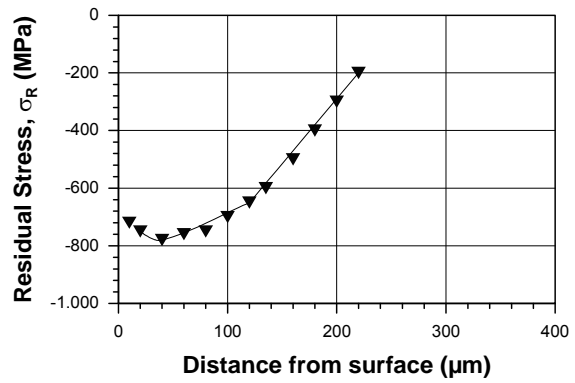


Fig. 12: Residual stress-depth profile

The S-N curves on Ti-2.5Cu are shown in Fig. 13 comparing the shot peened condition (SCCW14, 0.20 mmA) with an electropolished reference. Both fatigue life at high stress amplitudes as well as the HCF performance is strongly improved by shot peening (Fig. 13).

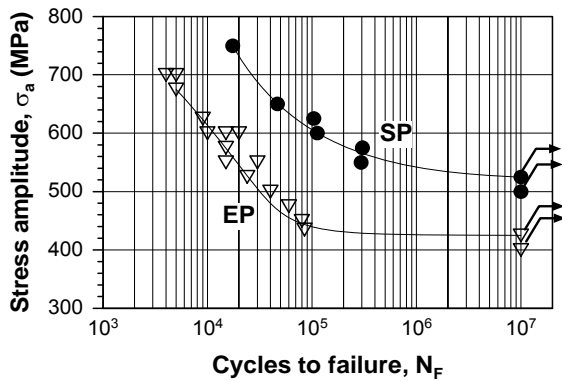


Fig. 13: S-N curves in rotating beam loading

Microhardness-depth profiles after shot peening of Ti-6Al-4V (SCCW14, 0,20 mmA) are illustrated in Figure 14 with corresponding residual stress-depth profiles plotted in Figure 15.

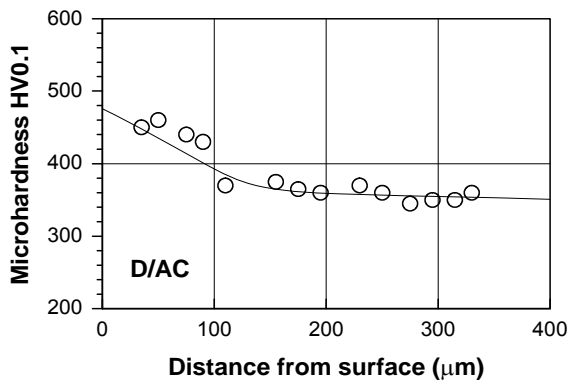


Fig. 14: Microhardness-depth profile

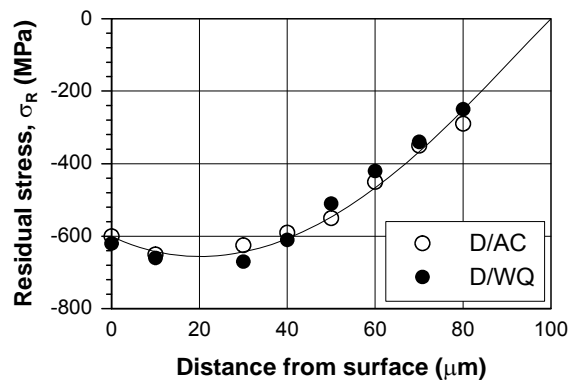
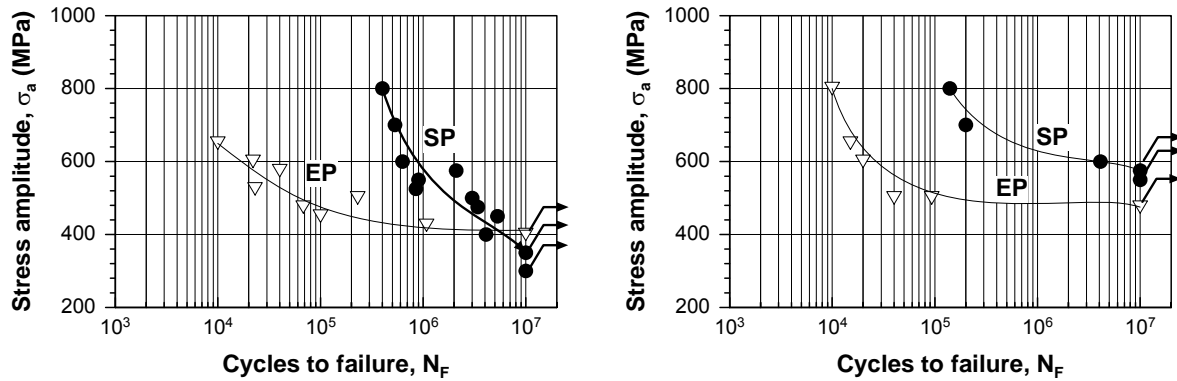


Fig. 15: Residual stress-depth profiles

Compared to the  $\alpha$  alloy Ti-2.5Cu, the hardness increase in Ti-6Al-4V is fairly small (compare Fig. 14 with Fig. 11) which corresponds to the limited work-hardening in this alloy as seen in Table 1. No difference in residual stress profiles was observed between D/AC and D/WQ (Fig. 15) this being the result of similar tensile properties (Table 1).

The S-N curves of these shot peened microstructures of Ti-6Al-4V are illustrated in Figure 16 where results on shot peened and electropolished conditions are plotted for D/AC (Fig. 15a) and D/WQ (Fig. 15b).

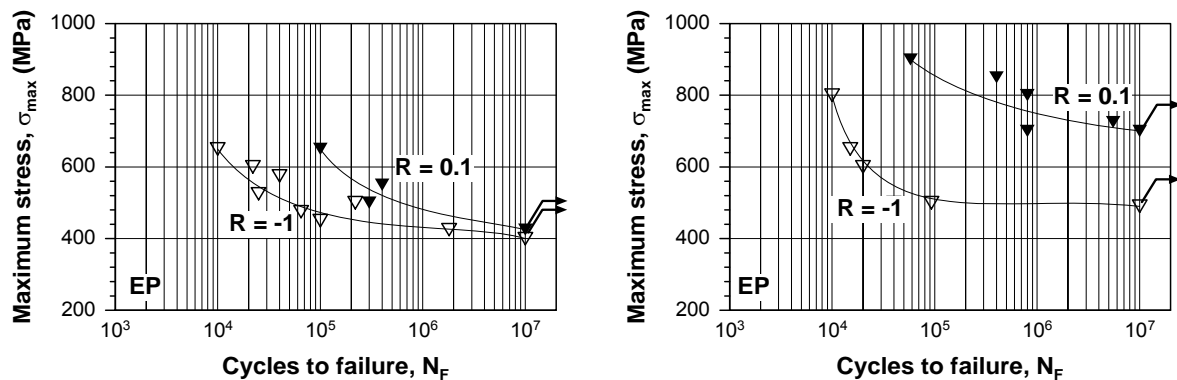


a) D/AC

b) D/WQ

Fig. 16: S-N curves in rotating beam loading ( $R = -1$ )

Obviously, D/AC exhibits a slight drop in HCF strength after shot peening (Fig. 14a) whereas the HCF strength is enhanced in D/WQ (Fig. 14b). These differences in HCF response to shot peening can be explained by the differences in mean stress sensitivities between D/AC and D/WQ as illustrated in Figure 16.



a) D/AC

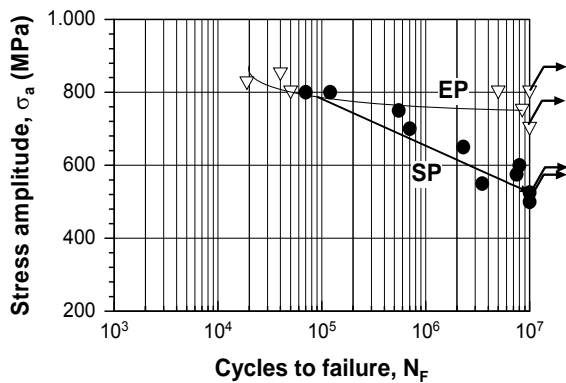
b) D/WQ

Fig. 17: S-N curves in rotating beam ( $R = -1$ ) and axial loading ( $R = 0.1$ )

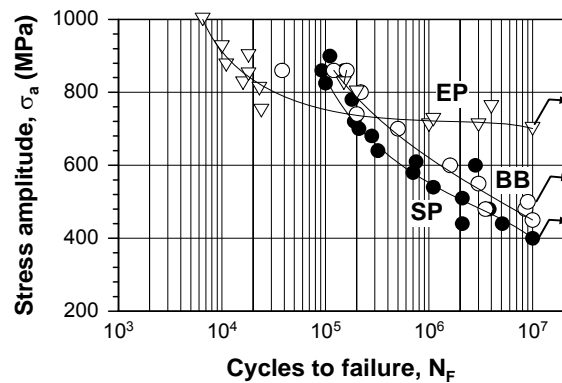
As seen in Figure 17, the sensitivity of D/AC to superimposed tensile stresses is much more pronounced than that of D/WQ. Since residual tensile stresses are the reason for the generally observed subsurface nucleation sites in mechanically surface treated titanium alloys, this anomalous mean stress sensitivity in D/AC (Fig. 17a) can explain the poor fatigue performance after shot peening (Fig. 16a).

The fatigue performance of the various strength levels of TIMETAL LCB are shown in Figure 18 illustrating the effects of shot peening (0.55 mmA) in comparison to ball-burnishing and electropolished baselines. As seen, highly aged conditions in TIMETAL LCB (Fig. 19 a, b) respond to shot peening with a marked loss in HCF

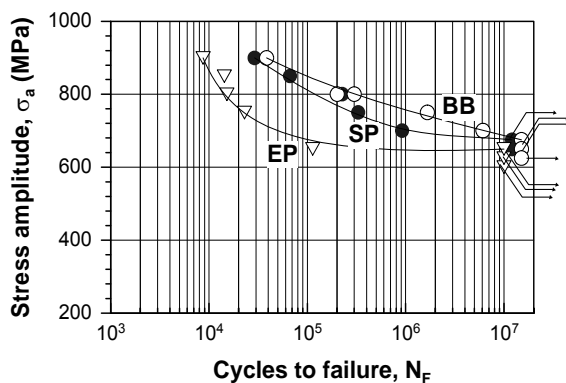
strength. Again, fatigue crack nucleation sites in shot peened specimens were generally found in subsurface regions.



a) aged 0.5 h at 500°C



b) pre-strained + aged 0.5h at 500°C



c) aged 8h 540°C

Fig. 19: S-N curves in TIMETAL LCB

Presumably, the drop in HCF strength is related to residual tensile stresses which can also explain the marked drop in HCF strength after ball-burnishing (Fig. 19 b). Interestingly, the lower strength condition in TIMETAL LCB (Fig. 19 c) does not show this marked deterioration of the HCF strength after shot peening or ball-burnishing. More work is needed to understand this behavior.

## ACKNOWLEDGEMENTS

The authors would like to thank the Deutsche Forschungsgemeinschaft DFG for financial support through contract WA 692/30-1. They would also like to thank T. Ludian and M. Kocan for performing the fatigue tests and residual stress measurements.

## REFERENCES

- G. R. Leverant, S. Langer, A. Yuen and S. W. Hopkins, *Met. Trans.* 10A (1979) 250.
- L. Wagner and G. Lütjering, *Shot Peening* (A. Niku Lari, ed.) (1982) 453.
- L. Wagner and C. Müller, *J. Materials Manufacturing & Processes* (1992) 423.
- L. Wagner, *Surface performance of Titanium Alloys* (J. K. Gregory, H. J. Rack and D. Eylon, eds.) TMS-AIME (1996) 199.
- M. Kocan, H. J. Rack and L. Wagner, *JMEPEG* (2005) 14: 765.